World Bulletin of Public Health (WBPH)
Available Online at: https://www.scholarexpress.net
Volume-35, June 2024
ISSN: 2749-3644

MRI AND CT IMAGE-BASED RADIOMICS DETECTION OF FUNCTIONAL LIVER RESERVE BEFORE SURGERY OR BIOPSY.

Turgunov B.Sh, Baratova G.Q, Mo'minova J.A, Soqiyev S.A

Article history:

Received: March 30th 2024
Accepted: April 26th 2024

Abstract:

Despite significant advances in all areas of medicine, particularly dentistry, the treatment of patients with chronic ostitis remains an urgent problem for both dentists and scientists.

The difficulties that arise in the treatment of periapical changes in chronic forms of ostitis are that tissue regeneration in the area of the root tip occurs 6-12-24 months after the end of endodontic treatment. Therefore, many scientists are developing new tools to stimulate and accelerate periapical regeneration processes and improving existing methods.

Keywords: Osteoplastic Materials, Bone Microporosity, Bone Macroporosity, Jawbone, Regeneration

INTRODUCTION

Primary liver cancer is the sixth most common cancer and is demonstrated to be the third contributing factor for global cancer death, showing about 906,000 new cases and 830,000 deaths in 2020 [1]. Among primary liver cancer cases, hepatocellular carcinoma (HCC) accounts for the most with about 75-85% [1]. Evidence has shown that Asia and Africa get the highest incidence of HCC in the world [2]. For HCC therapy, partial hepatectomy (PH) is still the optimal choice although most patients have reached an advanced stage because of insidious symptoms [3, 4]. However, it should be noticed that the post-hepatectomy liver failure (PHLF) is one of the important complications, and PHLF is the major cause of postoperative mortality. Normally the incidence of PHLF is 0.7- 9.1% and can reach 58.22% when the major hepatectomy is performed [5, 6]. Thus the presurgical evaluation of functional liver reserve seems critical and necessary as the accurate evaluation can help reduce the risk of hepatectomy and avoid PHLF.

In clinical work, liver volumetry and scoring systems based on blood tests, such as ALB, AST, TBIL, and indocyanine green retention at 15 min retention rate (ICG-R15) are classic indexes used for the evaluation of functional liver reserve. Liver volumetry can be obtained by 3D reconstruction technology [7]. The scoring systems contain the MELD score, Child-Turcotte-Pugh (CTP) score, and Albumin-bilirubin (ALBI) grade. By comparing the above indexes, the ICG-R15 has its own advantages. Firstly, it can help doctors detect functional liver reserve abnormality earlier and more accurately. Secondly, it has also been proven to have a positive correlation to liver failure and morbidity after hepatectomy [8]. The ICG-R15 values of the patient in different intervals (threshold: 10%, 20%, 30%) can affect and guide the selection of surgical treatment methods [9]. Thus, the ICG clearance test was considered to be the optimal evaluation of preoperative function liver reserve [10].

World Bulletin of Public Health (WBPH)
Available Online at: https://www.scholarexpress.net
Volume-35, June 2024
ISSN: 2749-3644

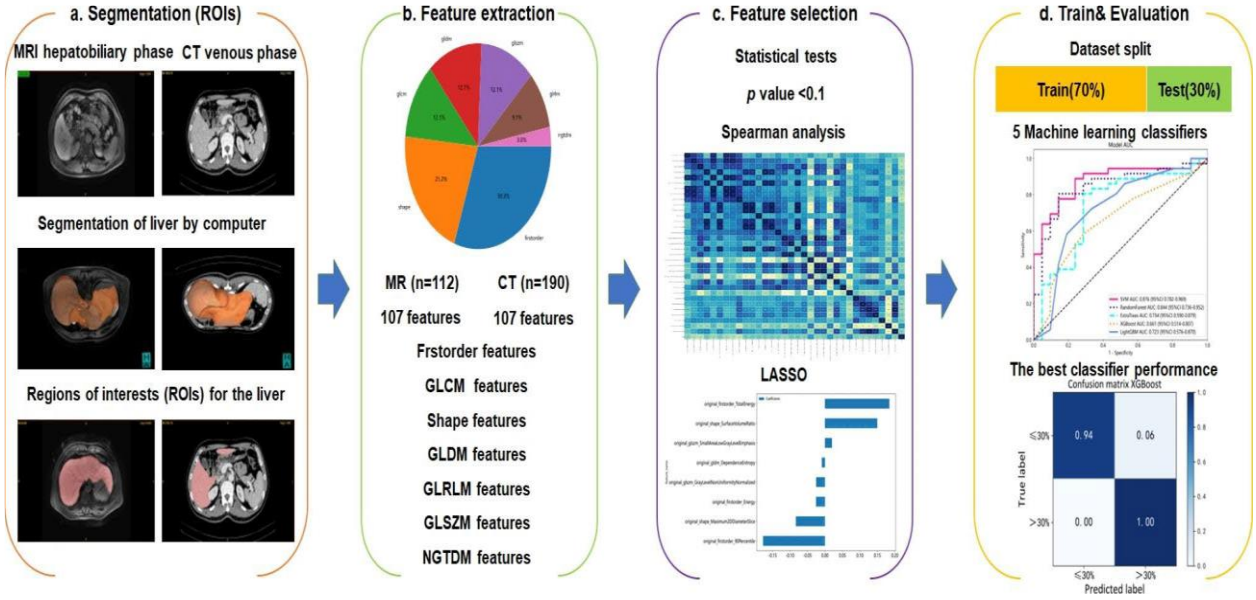

METHODS

Flowchart

According to the flowchart of this work (Fig. 1), the Gd-EOB-DTPA-enhanced hepatic MRI (MRI) data from 112 patients and contrast-enhanced CT (CT) data from 190 patients were retrospectively collected. The hepatobiliary phase at 15 min of MRI and the portal venous phase of CT were selected. Firstly, the ROI liver region was segmented, and the features were extracted from the MRI and CT images. Next, the features were further screened through the P-value and correlation coefficient. For radiomic model development, the dataset was randomly divided into a training dataset and a test dataset. The training dataset aimed to train the model.

Patients

By reviewing the patients who were diagnosed with HCC in our hospital from May 2017 to April 2022, the inclusion criteria were set as follows: (1) all patients were diagnosed as HCC; (2) Gd-EOB-DTPA-enhanced hepatic MRI or contrast-enhanced CT in all phases was completed within one week before treatment or surgery; (3) ICG clearance test was completed within one week before treatment or surgery; (4) patients without jaundice during ICG clearance test [18]; (5) all patients had no history of previous liver surgery or radiofrequency ablation(RFA). A total of 190 patients were included in this study. All the 190 patients have CT data while only 112 cases of them have both MRI data. Details are listed in Table 1.

MRI and CT acquisition

The Gd-EOB-DTPA-enhanced hepatic MRI examination and the contrast-enhanced CT examination were conducted by a Siemens Skyra 3.0 T MRI scanner and a Siemens SOMATOM Definition Flash scanner, respectively. Scans were performed from the top of the liver to the pelvis. The MRI scanning parameters were selected as below: the repetitiontime was 3.9 ms, the echotime was 1.4 ms, the matrix was 320 × 256, the field of view was 400 mm × 400 mm and the slice thickness was 3 mm. The Gd-EOB-DTPA (Primovist, Bayer Schering Pharma AG, Berlin, Germany) was used as a contrast agent for enhanced MRI scanning, and the contrast agent (with flow rate of 2.0 ml/s and dose of 0.1ml/kg) was injected through elbow vein using a high-pressure syringe.

Image segmentation

The computer-assisted surgery system (CAS) (CAS-Lv, Qingdao Hisense Medical Equipment Co., Ltd.) was used to segment the liver contour automatically from the hepatobiliary phase after 15 min of MRI and venous phase of the CT, to obtain the regions of interest (ROI) of the liver. For liver segmentation of MRI and CT, the Dice coefficient was more than 0.95 (this Dice coefficient is the manufacturer reference data of CAS-Lv).

Radiomic feature extraction

Before feature extraction, the images are normalized to reduce the voxel spacing variation effect and are resampled with voxel sizes of 1 mm × 1 mm × 1 mm. Parameters are set as follows: normalizeScale: 1000, interpolations: sitkNearestNeighbor, binWidth: 5. For the type of normalization, we adapt the Min-Max normalization method to scale the pixel values of the image. We extracted two radiomics feature sets from CT and MRI, respectively. Each feature set contains 107

World Bulletin of Public Health (WBPH)
Available Online at: https://www.scholarexpress.net
Volume-35, June 2024
ISSN: 2749-3644

features and was split into seven different groups: (1) first-order statistics of voxel intensity features (n = 18), (2) shape features (n = 14), (3) gray level co-occurrence matrix (GLCM) features (n = 24), (4) gray level dependence matrix (GLDM) features (n = 14), (5) gray level run-length matrix(GLRLM) features (n = 16), (6) gray level size zone matrix (GLSZM) features (n = 16), and (7) neighboring gray tone difference matrix (NGTDM) features (n = 5). The feature extraction process is conducted automatically by using the PyRadiomics package (Python version 3.7). Each feature was named by image type, feature group, feature name and concatenated underlines. For example, original_firstorder.

Radiomic feature selection

At first, for each feature, statistical t-test was performed to evaluate differences between different groups. When the two-tailed p-value of the feature was $p < 0.1$ [19–21], we consider this feature was significantly different between groups and then was retained. Second, to reduce the collinearity of features, spearman correlation analysis was performed. When the correlation coefficient between two features was $r>0.9$, one feature was randomly retained. At last, the LASSO algorithm was used to reduce the unimportant features and select the features with non-zero coefficient values.

Model construction and performance evaluation

Supervised learning was used for training and prediction. More specifically, five ML algorithms were applied to investigate the performance of the model, whereas these classifiers were Support Vector Machines (SVM), Extra-Trees (ET), Random Forest (RF), Light Gradient Boosting Machine (LightGBM) and eXtreme Gradient Boosting (XGBoost). All selected features were used as input to classify the evaluation of functional liver reserve (ICG-R15 ≤ 10% vs. ICG-R15>10%, ICG-R15 ≤ 20% vs. ICG-R15>20%, and ICG-R15 ≤ 30% vs. ICG-R15>30% as 2-class classifier). All patients were randomly split into two cohorts. One was called the training dataset (70%) and the other was called the test dataset (30%). Each model was trained on the training set and then made predictions by using the test set. A total of five models were constructed and compared with each other to find the best performing model. The ROC curves were used to calculate the AUC value which can evaluate the predictive power of these models. The cut-off values of sensitivity and specificity corresponding to the maximum value of the Youden index were calculated. The final prediction results include AUC (95% CI), ACC, sensitivity and specificity.

Statistical analysis

We used the statistical t-test and Chi-square test to analyze the between-group differences in clinical baseline characteristics (shown in Table 1). Statistical significance was defined as a two-sided p-value < 0.05 (see Supplementary Table S1-S6). Referring to the previous studies [19, 20], we used the statistical t-test to analyze and select the radiomics features with significance to be p-value < 0.1. For features with high repeatability, correlation analysis was performed by Spearman correlation analysis. One of the two features was randomly retained when the correlation coefficient between the two was larger than 0.9. Features were further selected by the LASSO method and were finally used to construct the model.

RESULTS

The features were selected by conducting statistical tests, spearman correlation analysis, and LASSO. And the final selected features and their corresponding LASSO coefficients derived from Gd-EOB-DTPA-enhanced hepatic MRI and contrast-enhanced CT are shown in Table 3.

Under functional liver reserve thresholds (ICG-R15 = 10%, ICG-R15 = 20% and ICG-R15 = 30%), five ML algorithms were used to construct the model and were trained on the training dataset. The trained models were then used to predict the result on the test dataset. The detailed performance of the five models is described in Table 4. For MRI groups, more specifically, the classifier XGBoost achieves the highest performance when ICG-R15 = 10% is used as a threshold, with AUC = 0.917 (95% CI: 0.823–1.000) and ACC = 0.882. Random Forest achieves the highest performance with AUC = 0.979 (95% CI: 0.941–1.000) and ACC = 0.882 at threshold ICG-R15 = 20%. For threshold ICG-R15 = 30%, the classifier XGBoost performs the best with AUC = 0.961 (95% CI: 0.890–1.000) and ACC = 0.941. Similar to the results for MRI groups, the classifier XGBoost for CT groups also achieves the best performance when threshold ICG-R15 = 10% (AUC = 0.822, 95% CI: 0.700–0.944, ACC = 0.842), and ICG-R15 = 30% (AUC = 0.938, 95% CI: 0.824–1.000, ACC = 0.965). Under threshold ICG-R15 = 20%, the classifier SVM is observed to perform the best with an AUC value of 0.860 (95% CI: 0.758–0.963) and ACC of 0.842. The detailed information of the best models is listed in Table 5.

The model confusion matrices and ROC curves are shown in Figs. 2 and 3, respectively. All AUC values are greater than 0.89 for the test dataset from MRI and are greater than 0.82 for the test dataset from CT. The results indicate that both MRI-based and CT-based ML models can achieve the goal of classification in

World Bulletin of Public Health (WBPH)
Available Online at: https://www.scholarexpress.net
Volume-35, June 2024
ISSN: 2749-3644

distinguishing the different values of ICG-R15 to some extent, which is promising to become an additional method to predict the functional liver reserve.

DISCUSSION

Radiomics has shown great value in the diagnosis and therapy of multiple diseases. We consider whether it is possible to use the radiomics method to perform an accurate assessment of functional liver reserve based on Gd-EOB-DTPA-enhanced hepatic MRI and contrast-enhanced CT in HCC patients. Under this perspective, MRI-based and CT-based ML models are developed and validated for distinguishing patients with functional liver reserves of different states. Our results demonstrate that both MRI-based and CT-based models worked satisfactorily in the aspect of the assessment of functional liver reserve. Recently, there has been an increasing application of imaging techniques in measuring the hepatic function in HCC patients, because it can provide more significant clinical information than an overall assessment [22]. For example, previous studies based on medical image analysis have demonstrated that liver has regional differences in hepatic parenchymal abnormalities [23, 24]. One recent work from Zhaoqi Shi et al. shows that radiomics analysis can be applied in the preoperative assessment of functional liver reserve in HCC patients [25]. However, this research only focused on Gd-EOB-DTPA-enhanced hepatic MRI to predict the ICG classification value to evaluate liver function in HCC patients, and the functional liver reserve thresholds are set to be ICG-R15 = 10%, ICG-R15 = 15%, and ICG-R15 = 20%. However, several limitations should be mentioned in our study. Firstly, the provided research images were obtained from our center, more patients are needed in order to achieve external cohort validation. The baseline characteristics and features from a single center may not conform to the population. Secondly, the analysis of functional liver reserve under specific thresholds is a 2-class classification problem, which cannot cover all of the clinically significant ICG-R15 value intervals mentioned in the Makuuchi criteria for safe hepatic resection [9]. Thirdly, regarding the fact that some patients had CT scans but no MRI scans, we did not make the multimodality evaluation with CT and MRI. In the future, the classification with massive patients and multi-center data will be investigated by different ICG value intervals and multi-class classification methods. The multimodality evaluation with CT, MRI and clinical data will be a focus for our follow-up studies.

CONCULSION

Both MRI-based and CT-based ML models are shown to achieve the goal of classification in distinguishing the different values of ICG-R15 to some extent, which are proved to be valuable methods for functional liver reserve evaluation. Among the five classifiers, XGBoost was demonstrated to perform best. Our work provides valuable insights, which can help clinicians to construct an effective prediction model and develop personalized precision treatment strategies.

Abbreviations

ACC Accuracy
AST Aspartate aminotransferase
ALT Alanine transaminase
PT Prothrombin time
CT Computed tomography
CI Confidence intervals
MRI Magnetic resonance imaging
HCC Hepatocellular carcinoma
RFA Radiofrequency ablation
ET Extra-Trees
Gd-EOB-DTPA Gadolinium ethoxybenzyl dimeglumine
ML Machine learning
ICG-R15 Indocyanine green retention rate at 15 min
ROI Regions of interest
RF Random Forest
AUC Area under the ROI curve
ROC Receiver operating characteristic
BMI Body Mass Index
HBV Hepatitis B Virus
ALB Albumin
TBIL Total Bilirubin
GGT Gamma-glutamyltransferase

REFERENCES

1. Akhmedov YA, Ataeva SKh, Ametova AS, Bazarova SA, Isakov HKh THE HISTORY OF THE DEVELOPMENT OF RADIATION DIAGNOSTICS. Web of scientist: International scientific research journal. 2021;2:34-42.
2. Akhmedov YA, Rustamov UKh, Shodieva NE, Alieva UZ, Bobomurodov BM Modern Application of Computer Tomography in Urology. Central Asian journal of medical end natural sciences. 2021;2(4):121-125.
3. Ataeva SKh, Ravshanov ZKh, Ametova AS, Yakubov DZh Radiation visualization of chronic joint diseases. Central Asian journal of medical end natural sciences. 2021;2(2):12-17

World Bulletin of Public Health (WBPH)
Available Online at: https://www.scholarexpress.net
Volume-35, June 2024
ISSN: 2749-3644

4. Hamidov OA, Diagnostics of injuries of the soft tissue structures of the knee joint and their complications. European research. Moscow. 2020;1(37):33-36.
5. Khamidov OA, Khodzhanov IYu, Mamasoliev BM, Mansurov DSh, Davronov AA, Rakhimov AM The Role of Vascular Pathology in the Development and Progression of Deforming Osteoarthritis of the Joints of the Lower Extremities (Literature Review). Annals of the Romanian Society for Cell Biology, Romania. 2021;1(25):214 – 225
6. Khamidov OA, Akhmedov YA, Ataeva SKh, Ametova AS, Karshiev BO Role of Kidney Ultrasound in the Choice of Tactics for Treatment of Acute Renal Failure. Central Asian journal of medical end natural sciences. 2021;2(4):132-134
7. Khamidov OA, Akhmedov YA, Yakubov DZh, Shodieva NE, Tukhtaev TI DIAGNOSTIC POSSIBILITIES OF USES IN POLYKYSTOSIS OFKIDNEYS. Web of scientist: International scientific research journal. 2021;2(8):27-33
8. Khamidov OA, Ataeva SKh, Ametova AS, Yakubov DZh, Khaydarov SS A Case of Ultrasound Diagnosis of Necrotizing Papillitis. Central Asian journal of medical end natural sciences. 2021;2(4):103-107
9. Khamidov OA, Ataeva SKh, Yakubov DZh, Ametova AS, Saytkulova ShR ULTRASOUND EXAMINATION IN THE DIAGNOSIS OF FETAL MACROSOMIA. Web of scientist: International scientific research journal. 2021;2(8):49-54
10. Khamidov OA, Mirzakulov MM, Ametova AS, Alieva UZ Multispiral computed tomography for prostate diseases. Central Asian journal of medical end natural sciences. 2021;2(2):9-11
11. Khamidov OA, Normamatov AF, Yakubov DZh, Bazarova SA Respiratory computed tomography. Central Asian journal of medical end natural sciences. 2021;2(2):1-8
12. Khamidov OA, Urozov UB, Shodieva NE, Akhmedov YA Ultrasound diagnosis of urolithiasis. Central Asian journal of medical end natural sciences. 2021;2(2):18-24
13. Khamidov OA, Yakubov DZh, Alieva UZ, Bazarova SA, Mamaruziev ShR Possibilities of Sonography in Differential Diagnostics of Hematuria. Central Asian journal of medical end natural sciences. 2021;2(4):126-131
14. Khamidov OA, Yakubov DZh, Ametova AS, Bazarova SA, Mamatova ShT Application of the Ultrasound Research Method in Otorhinolaryngology and Diseases of the Head and Neck Organs. International Journal of Development and Public Policy. 2021;1(3):33-37
15. Khamidov OA, Yakubov DZh, Ametova AS, Turdumatov ZhA, Mamatov RM Magnetic Resonance Tomography in Diagnostics and Differential Diagnostics of Focal Liver Lesions. Central Asian journal of medical end natural sciences. 2021;2(4):115-120
16. Rustamov UKh, Shodieva NE, Ametova AS, Alieva UZ, Rabbimova MU US-DIAGNOSTICS FOR INFERTILITY. Web of scientist: International scientific research journal. 2021;2(8):55-61
17. Rustamov UKh, Urinboev ShB, Ametova AS Ultrasound diagnostics of ectopic pregnancy. Central Asian journal of medical end natural sciences. 2021;2(2):25-28
18. Abdurakhmanovich, K. O., & ugli, G. S. O. (2022). Ultrasonic Diagnosis Methods for Choledocholithiasis. Central Asian Journal Of Medical And Natural Sciences, 3(2), 43-47.
19. Abdurakhmanovich, K. O., & ugli, G. S. O. (2022). Ultrasound Diagnosis of the Norm and Diseases of the Cervix. Central Asian Journal Of Medical And Natural Sciences, 3(2), 58-63.
20. Yakubov Doniyor Javlanovich, Juraev Kamoliddin Danabaevich, Gaybullaev Sherzod Obid ugli, and Samiev Azamat Ulmas ugli. 2022. "INFLUENCE OF GONARTHROSIS ON THE COURSE AND EFFECTIVENESS OF TREATMENT OF VARICOSE VEINS". Yosh Tadqiqotchi Jurnali 1 (4):347-57.
21. Yakubov , J., Karimov , B., Gaybullaev , O., and Mirzakulov , M. 2022. Ultrasonic and radiological picture in the combination of chronic venous insufficiency and osteoarthritis of the knee joints. Academic Research in Educational Sciences. 5(3), pp.945–956.
22. Yakubov D. Z., Gaybullaev S. O. The diagnostic importance of radiation diagnostic methods in determining the degree of expression of gonarthrosis //UZBEK JOURNAL OF CASE REPORTS. – С. 36.
23. Якубов Д. Ж., Гайбуллаев Ш. О. Влияние посттравматической хондропатии на функциональное состояние коленных суставов у спортсменов. Uzbek journal of case reports. 2022; 2 (1): 36-40. – 2022.
24. Alimdjanovich, R.J., Obid , K., Javlanovich, Y.D. and ugli, G.S.O. 2022. Advantages of Ultrasound Diagnosis of Pulmonary Pathology

World Bulletin of Public Health (WBPH)
Available Online at: https://www.scholarexpress.net
Volume-35, June 2024
ISSN: 2749-3644

in COVID-19 Compared to Computed Tomography. Central Asian Journal of Medical and Natural Science. 3, 5 (Oct. 2022), 531-546.
25. Kadirov J. F. et al. NEUROLOGICAL COMPLICATIONS OF AIDS //Journal of new century innovations. – 2022. – T. 10. – №. 5. – C. 174-180.